Geophysica (1995), 31(2), 31-45

Modeling the Influence of Ice on Sea Level Variations in the Baltic Sea

Zhan-hai Zhang[1] *and Matti Leppäranta*[2]

1 National Research Center for Marine Environment Forecasts, No.8, Da Hui Si, Haidian District, 100081 Beijing, China
[2] Department of Geophysics, P.O. Box 4, FIN-00014 University of Helsinki, Finland

(Received: February 1995; Accepted: June 1995)

Abstract

The influence of sea ice on wind-driven sea level variations is examined. A coupled ice-ocean model is used to simulate the evolution of the sea level elevation in different ice conditions in the Baltic Sea; a simple analytical model is utilized to aid the interpretation. Ice cover highly modifies the air-sea kinetic energy transfer. Water piling-up is decreased as a result of internal friction within the ice cover: in ice-covered cases the sea surface slope may be as low as one-third of the ice-free value in similar wind conditions. The results fairly well agree with observations. Besides reducing the changes in the sea level, the ice cover also affects the current field. For severe ice conditions the current field magnitude dropped to 20 % from the ice-free case.

Key words: sea ice, ice-ocean model, sea level variation

1. Introduction

In freezing seas the wind-driven circulation of water is highly affected by the extent and strength of the ice pack. By transmitting the wind forcing to the sea water, the ice may increase or decrease the kinetic energy input into the sea. The increase is true for free drifting rough ice which normally has a higher wind drag coefficient than ice-free water; on the other hand, no energy gets through the ice when the ice cover is stationary because of its high internal friction. As a consequence of the circulation the water level variations become modified by the ice.

In the Baltic Sea, wind stress is the principal force for the circulation and piling-up of water. Tides are very small, the amplitude being less than 1 cm. Ice occurs annually in the region. The ice cover is dynamic; strong winds break the ice, opening up leads and building up ridges in the pack. The mobility of the ice in any of the Baltic basins rapidly decreases as the basin becomes totally ice-covered and the ice gets thicker.

The reducing influence of ice on the wind-driven water piling-up in the Baltic Sea winter was first reported by *Lisitzin* (1957). She examined the Kemi-Vaasa water level difference in the Gulf of Bothnia and found that this difference became damped down to

Published by the Finnish Geophysical Society, Helsinki

1/3 from ice-free cases in severe ice seasons (Figs. 1-2). This damping is due to internal friction which uses much of the wind energy input in the ice deformation (*Leppäranta*, 1981). *Omstedt* and *Nyberg* (1991) further examined sea level statistics and obtained a maximum ice damping factor of 1/2 for the water level slope.

The role of sea ice in winter time circulation and water piling-up is examined in this work using a coupled ice-ocean dynamics model. The raw results have been given in *Zhang* and *Leppäranta* (1992) and are further analysed here. The area of study is the Bay of Bothnia, the northern basin of the Gulf of Bothnia (Fig. 1). A simple analytic analysis is first performed. With the full model selected cases with different ice conditions are simulated and the results are compared with the observed data. In addition, the possibility of using this coupled model for predicting water level in winter months is tested.

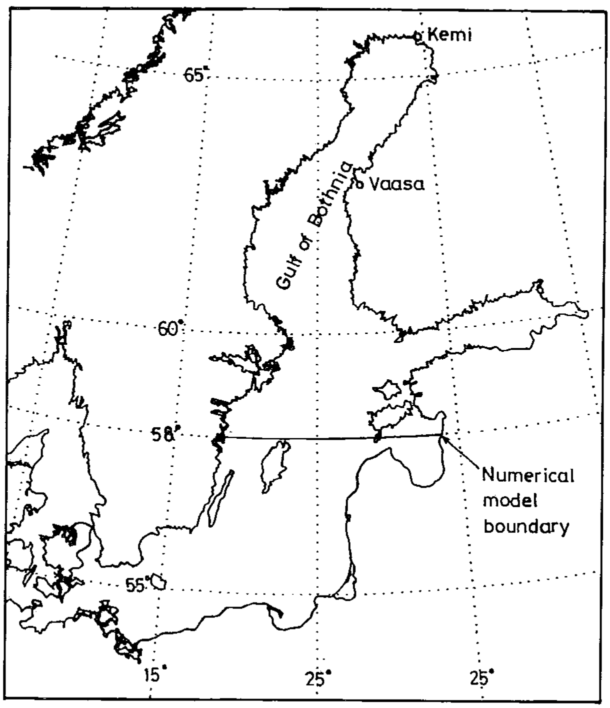

Fig. 1. The Gulf of Bothnia, divided (at about the Vaasa level) into the Bay of Bothnia and the Sea of Bothnia.

2. *Analytic analysis*

Consider a long channel aligned with the x-axis and closed at $x = L$. Assume also that the wind is constant and blows in the positive x-direction. The steady state balance between the wind stress and pressure gradient gives the sea surface slope (e.g. *Lisitzin*, 1957):

$$b = \tau_{aw}/(\rho g d) \quad (1)$$

where τ_{aw} is the wind stress on the water, ρ is the water density, g is the acceleration of the gravity, and d is the water depth. The wind stress law is parametrized as

$$t_{aw} = \rho_a C_{aw} |U_a| U_a \,, \quad (2)$$

where ρ_a is air density, C_{aw} is air-water drag coefficient, and U_a is wind velocity. For neutral stratification, the drag coefficient was given by *Garratt* (1977) as $C_{aw} = (0.75 + 0.067\, U_a) \times 10^{-3}$.

Now add an ice cover with compactness A and mean thickness h to the system. The wind stress on ice is $\tau_{ai} = \rho_a C_{ai} |U_a| U_a$ where C_{ai} is the air-ice drag coefficient; for the Baltic Sea $C_{ai} = 1.8 \times 10^{-3}$ (*Joffre*, 1984; *Leppäranta* and *Omstedt*, 1990). The wind stresses over ice and water then become equal at $U_a = 15.7$ m/s. The ice-water stress is given by

$$t_{iw} = \rho C_{iw} |u-U|(u-U) \,, \quad (3)$$

where C_{iw} is the ice-water drag coefficient and u and U are the ice and water velocities. A representative value for the drag coefficient is $C_{iw} = 3.5 \times 10^{-3}$ in the Baltic Sea (*Leppäranta* and *Omstedt*, 1990). Finally the stress driving the water circulation becomes

$$t_w = A\tau_{iw} + (1-A)\tau_{aw} \,. \quad (4)$$

For the channel flow, a one-dimensional ice dynamics description can be easily obtained from *Hibler's* (1979) model:

$$r_i h\, (\partial u/\partial t + u\, \partial u/\partial x) = A\tau_{ai} - A\tau_{iw} + \partial\sigma/\partial x \quad (5a)$$

$$ûA/\partial t = -\partial(Au)/\partial x \,, \ 0 \leq A \leq 1 \quad (5b)$$

$$ûh/\partial\tau = -\partial(hu)/\partial x \quad (5c)$$

where ρ_i is the ice density, and σ is the internal ice stress given here by the plastic law

$$s = -P_* h \exp\{-C(1-A)\}, \qquad \partial u/\partial x < 0 \quad (6)$$

$$s = 0 \,, \qquad \partial u/\partial x \geq 0$$

with P_* and C being ice strength constants. The sea surface slope term for the ice drift is small, even in the water piling-up cases, and has been neglected in this study (slope term

$= \rho_i h\, g{\cdot}\beta \sim 10^3 \cdot 1 \cdot 10 \cdot 10^{-6}$ N/m^2 = 10^{-2} N/m^2 $<< \tau_a$). The boundary conditions are such that at the ice edge the ice stress is zero and at $x = L$ the ice velocity is zero.

In the present case the only steady-state solution of Eqs. (5) is $u \equiv 0$ which leads to $U \equiv 0$ (no forcing) and consequently to $\beta \equiv 0$. The time scale for the full adjustment is however long (*Leppäranta* and *Hibler*, 1985), much longer than the wind set-up time scale of one day or so. We may however consider the quasi-steady case of Eqs. (5) where the left-hand sides are equal to zero. This case is valid for the one-day time scale solution. The solution must be interpreted as a representative "mean" field (u, A, h) during the wind set-up process.

In this quasi-steady case the momentum equation gives us $A\tau_{iw} = A\tau_{ai} + \partial\sigma/\partial x$. Now using Eq. (4) for the surface stress on the water surface, the sea surface slope becomes

$$\mathrm{b} = [A\tau_{ai} + \partial\sigma/\partial x + (1\text{-}A)\tau_{aw}]/(\rho g d) \tag{7}$$

Integrating this formula from a point (within the ice pack) x=L_o to the solid boundary x=L gives the water level difference ΔH between these points:

$$\mathrm{D}H = \beta(L\text{-}L_o) = [(L\text{-}L_o)\overline{A}\tau_{ai} + (L\text{-}L_o)(1\text{-}\overline{A})\tau_{aw} + \sigma(L)\text{-}\sigma(L_o)]/(\rho g d) \tag{8}$$

where the overbar stands for spatial averaging. If the wind is strong enough the ice moves and the ice stress equals the yield stress; otherwise the ice is motionless the ice stress balancing the wind forcing. Now take the strong wind case, and assume for simplicity that the ice field gets well packed so that $A \approx 1$ and choose L_o to be the ice edge; then $\sigma(L)$ = $-P_* h(L)$ and $\sigma(L_o) = 0$. The sea level difference between x=L and x=L_o is

$$\mathrm{D}H = [(L\text{-}L_o)\rho_a C_{ai}|U_a|U_a \text{-} P_* h(L)]/(\rho g d)\ . \tag{9}$$

For comparison, the ice free case gives

$$\mathrm{D}H = (L\text{-}L_o)\rho_a C_{aw}|U_a|U_a/(\rho g d). \tag{10}$$

This result differs qualitatively from *Lisitzin* (1957) in that the ice case does not go to zero parabolically but is cut to zero at about wind speed 14 m/s due to the ice strength. The comparison is shown in Fig. 2, assuming that $C_{aw} \approx C_{ai}$. The zero cut point gives us an estimate for the ice strength $P_* \approx 10^5$ N/m^2 in severe ice conditions.

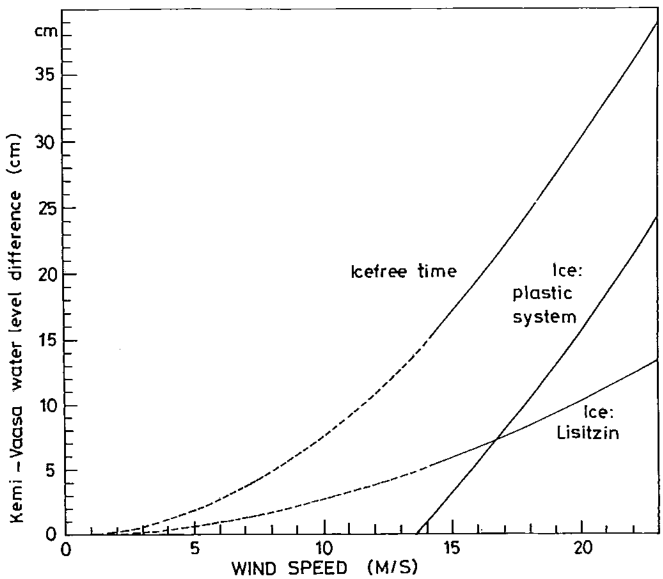

Fig. 2. The sea surface difference between Kemi and Vaasa, Gulf of Bothnia. "Ice free time" and "Ice: Lisitzin" are fits to observed data for wind speeds greater than 14 m/s by Lisitzin (1957); "Ice: plastic system" is an analytic model result fitted to Lisitzin's ice cases.

3. *Numerical model*

3.1 Model equations

A more complete treatment of the ice cover influence on sea level variations is obtained using a coupled ice-ocean dynamics numerical model. In the ice model the momentum equation is in the steady state form and a three level description is used for the ice thickness. The ocean model part is a two-dimensional one-layer model (*Zhang* and *Wu*, 1990b).

The ice model equations are

$$\nabla \cdot \sigma + A\tau_{ai} - A\tau_{iw} - \rho_{ih} f \mathbf{k} \times \mathbf{u} = 0 \qquad (11a)$$

$$\partial/\partial t\,(A, h_u, h_d) = -\mathbf{u} \cdot \nabla(A, h_u, h_d) + (\psi_A, \psi_u, \psi_d)\,,\ 0 \leq A \leq 1 \qquad (11b)$$

where f is the Coriolis parameter, **k** is unit vector vertically upward, h_u and h_d are the thicknesses of undeformed and deformed ice, respectively ($A[h_u + h_d] = h$), and (ψ_A, ψ_u, ψ_d) is the mechanical thickness redistributor. The ice stress is given by the *Hibler* (1979) viscous-plastic law. The ocean model equations are

$$\partial U/\partial t + U \cdot \nabla U + f\mathbf{k} \times U =$$

$$-g \nabla\zeta - \nabla p_a/\rho + [(1-A)\tau_{aw} + A\tau_{iw} + \tau_b]/\rho(d+\zeta) \tag{12a}$$

$$\partial\zeta/\partial t + \nabla\cdot[(d+\zeta)U] = 0 \tag{12b}$$

where ζ is the elevation of free surface, p_a is the air pressure at the sea surface, and τ_b is the bottom friction stress. Note that U is now the vertically integrated average current velocity.

The coupling between ice and ocean is described by the tangential stress on the ice/water interface which in the two-dimensional case is

$$t_{iw} = \rho C_{iw} |\boldsymbol{u} - \boldsymbol{U}| \{\cos\theta\,(\boldsymbol{u} - \boldsymbol{U}) + \sin\theta\,\mathbf{k}\times(\boldsymbol{u} - \boldsymbol{U})\} \tag{13}$$

where C_{iw} is the ice-water drag coefficient, and θ is the turning angle in the water (17°: *Leppäranta* and *Omstedt*, 1990). Note that τ_{iw} drives the sea while $-\tau_{iw}$ drives the ice. The air-sea and air-ice stresses generalize directly to two dimensions from the one-dimensional forms in section 2. The bottom stress is given by

$$t_b = -\rho_w g\, C^{-2}\, |U| U \tag{14}$$

where C is the Chezy coefficient $C = 1/n\ (d+\zeta)^{1/6}$ with $n = 0.02$ s m$^{-1/3}$ the Manning coefficient (see, e.g., *Li* and *Lam*, 1964).

The air pressure term was neglected in Eq. (12a); this term is not so relevant for the present wind setup study as the ice cover adjusts passively to hydrostatic sea level changes.

The open sea boundary is fixed along the 58°N latitude (see Fig. 1). At both open water and land boundaries the ice velocity and mass are zero. The numerical solution is obtained using a finite-difference technique. When integrating the oceanic part, the ice variables are kept fixed and vice versa.

In the ice model the spatial discretization is made in an Arakawa 'B' type grid; the grid size is 10 nautical miles and the time-step is 6 hours. The details of numerical methods in the ice model are found in *Hibler* (1979) and *Leppäranta* and *Zhang* (1992). The solution of the ocean model is obtained by the ADI numerical integration procedure (*Peaceman* and *Rachford*, 1955). The grid configuration is an Arakawa 'C' type grid. The grid size is the same as in the ice model and the time step is half an hour.

In the ice model there is an internal moving horizontal ice/water boundary (ice edge); there the internal ice stress is assumed to be zero. The velocity of fast ice is taken as zero and its concentration is one. In the ocean model, on the coast the normal velocity is zero. Due to the lack of information of the sea level elevation in the open boundary, a clamped boundary condition is used, i.e. the elevation of the free surface is assumed to be equal to zero. This boundary condition allows fluid flux across the boundary but does not permit the adjustment of the free surface. The assumption is reasonable for a deep region. In addition, because the analysis of results is mainly focused on the northern basin of the Gulf of Bothnia (see Fig. 1), the effect of the open boundary is relatively unnoticeable in a short time-scale.

In the ADI procedure, the solution is obtained through a two-step process in one timestep (*Zhang* and *Wu*, 1990a). In the first half-timestep, the continuity equation and the U-component momentum equation are solved simultaneously with implicit spatial differences for the first x-derivative. Then we obtain the linear equations for U and ζ at the time $t + \Delta t/2$:

$$a_1 U_{i,j} + b_1 \zeta_{i+1/2,j} + c_1 U_{i+1,j} = d_1 \tag{15a}$$

$$a_2 \zeta_{i+1/2,j} + b_2 U_{i+1,j} + c_2 \zeta_{i+1,j} = d_2 \tag{15b}$$

Here a_i, b_i, c_i, and d_i are known quantities which depend on the variables U, V and ζ at the previous time steps t-Δt and t. For a fixed index j, the coefficient matrix of the Eqs. (15) is tridiagonal, and it can be solved using a simple Gaussian elimination procedure. The velocity component V is calculated by explicitly integrating the V-component momentum equation. In the second half-timestep, the continuity equation and V-component momentum equation are simultaneously solved with implicit differences for the first y-derivative. Then a similar procedure as in the first half-timestep is performed.

3.2 Cases

The initial ice data consisted of compactness and thickness obtained from the ice maps of the Finnish Institute of Marine Research (*FIMR*, 1982, 1984, 1990). The initial velocities and the sea level elevation are zero. The wind fields were available four times per day (00, 06, 12 and 18 GMT) based on estimates of regional surface wind (10 regions in the Baltic Sea) given by the Finnish Meteorological Institute (FMI); they were linearly interpolated into every hour for the ocean model. The sea level data are hourly values from the FIMR stations at Kemi and Vaasa, shown in graphical form in *Zhang* and *Leppäranta* (1992). The wind and sea level data have been archived by FIMR.

Selected cases with different ice conditions and strong wind were simulated from the period 1982-1990. On the basis of the ice conditions these cases can be divided into three classes: I = the Gulf of Bothnia fully ice-covered, II = the Bay of Bothnia fully ice covered, and III = ice only in the Bay of Bothnia and coverage less than 50 %. In the analysis below, one typical case for each ice class is considered (see Fig. 3):

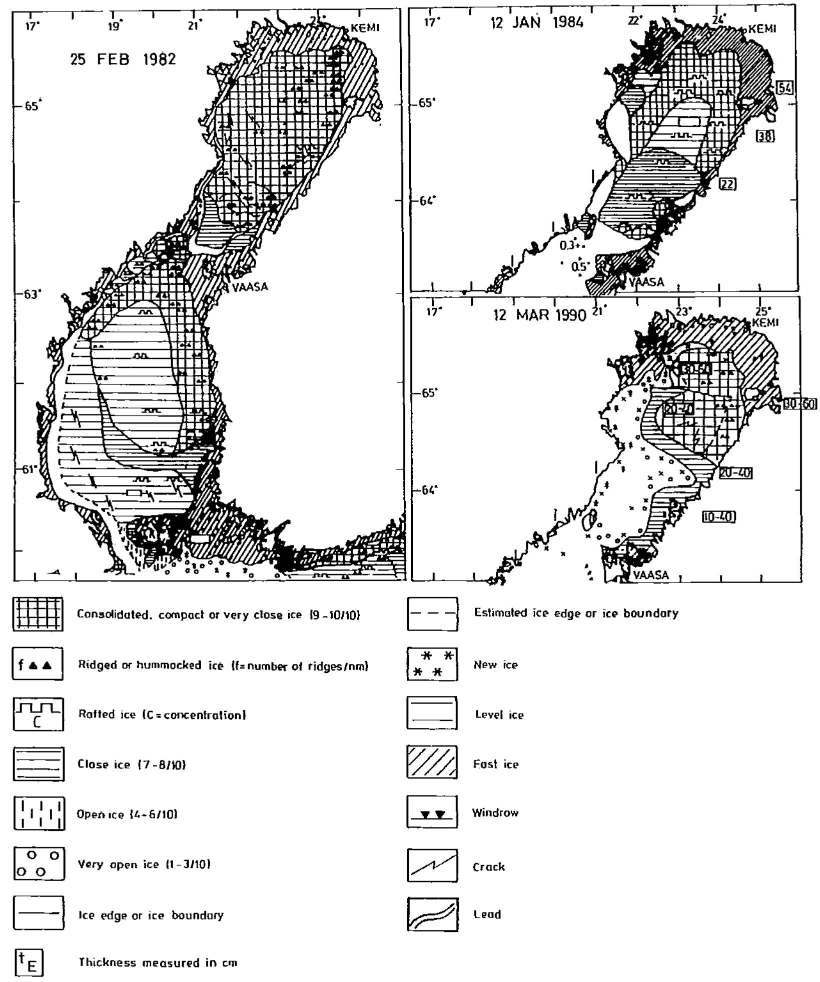

Fig. 3. The initial ice situations in the Gulf of Bothnia for the three study cases.

Case 1 [Ice class I]	25 Feb - 2 Mar 1982
Case 2 [Ice class II]	12 - 17 Jan 1984
Case 3 [Ice class III]	12 - 17 Mar 1990

The FIMR routine ice charts and sea level data were used for the validation of the model calculations. The average wind data from FMI for the Bay of Bothnia are given in Fig. 4. In case 1 the maximum wind speed was 14 m/s, 18 m/s in case 2, and 15 m/s in case 3.

Model runs were performed with the full coupled ice-ocean model and, for comparisons, with an "ice-free" model where the ice cover was totally ignored. The difference between these two kind of model runs gives information about modifications due to the ice on circulation and sea level changes.

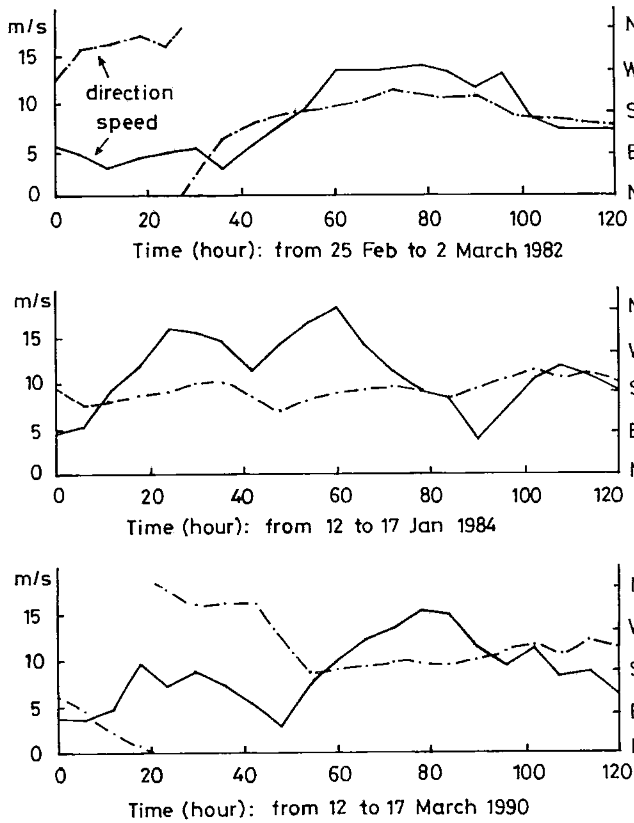

Fig. 4. Wind speed and direction in the study cases.

3.3 Results from numerical model

The evolution of the sea level elevation (Fig. 5) illustrates the fact that the coupled model is much closer to the observed data than the ice-free model. Note that the zero reference sea level is different in the model and observed data because the model calibration was not necessary here; one should note the changes in the curves and ignore the absolute level. Besides being weakened the peak of the elevation as a rule is also delayed due to the ice. The stronger the wind the more evident is the ice caused damping of the water level, and the wider the ice cover the more notable is the water level decrease.

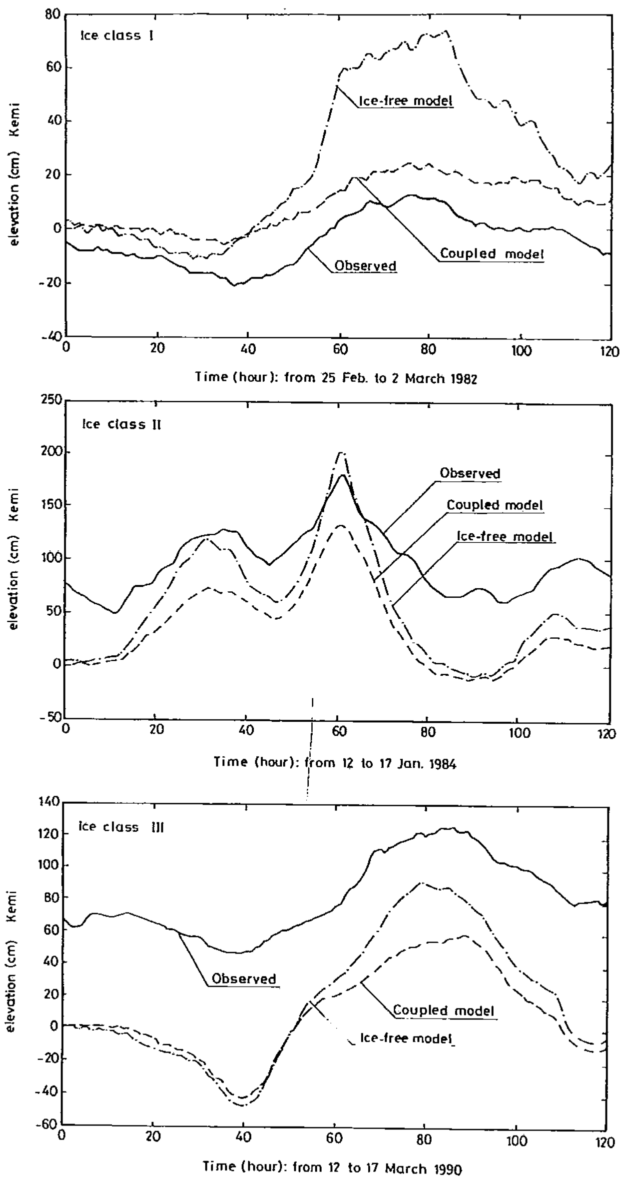

Fig. 5. Time series of the sea level elevation in Kemi.

The spectra of time series of the sea level elevation were calculated, and the result for case 1 is shown in Fig. 6. The spectral density peaks at low frequencies; over 95 % of the total variance is at less than 0.04 cycles per hour (cph) ≈ 1 cycle per day. It can be seen that the agreement between the coupled model and the observed data is quite good. The spectral level decreases substantially due to the presence of the ice.

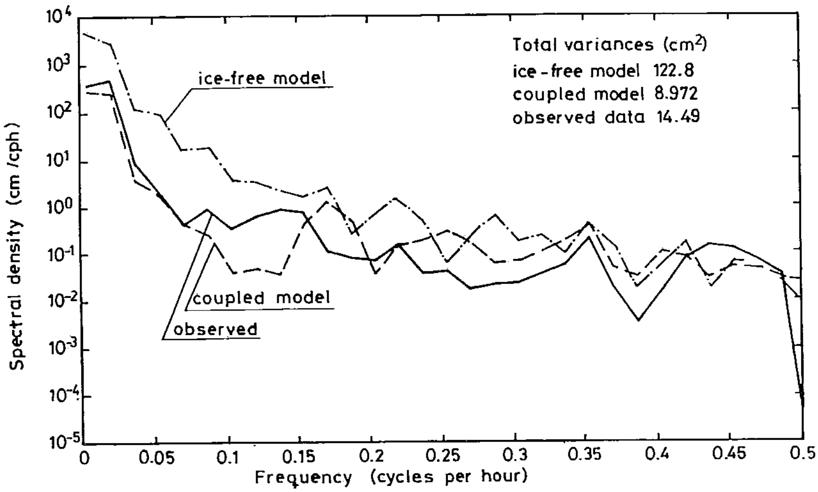

Fig. 6. The spectra of the sea level elevation in Kemi from 25 February to 2 March 1982 (case 1).

The calculations for the water piling-up between Kemi and Vaasa are shown in Fig. 7. In cases 1 and 2 the coupled model agrees quite well with the observations while the ice-free model shows considerably different output. The reducing influence of ice on water is thus seen clearly. The influence is remarkable for strong winds but not noticeable for weak winds. In case 1 (severe ice situation) the ice-caused slope reduction factor was 0.4, a bit larger than the Lisitzin's factor of 1/3. In case 2 this factor was 0.65. Case 3 looks a bit strange and there may be problems with the wind data. But even here, comparing the outputs of the two models, the reduction factor appears to be about 0.65.

The influence of sea ice on current fields was pronounced. The model velocity fields from case 1, averaged for the strong wind period (24 hours), are given in Fig. 8. It is seen that the speed is decreased by a factor of five when the ice cover is included. Also the current direction is modified by the ice. The maximum damping in the current is found in the fast ice areas, while near the ice edge the changes are small.

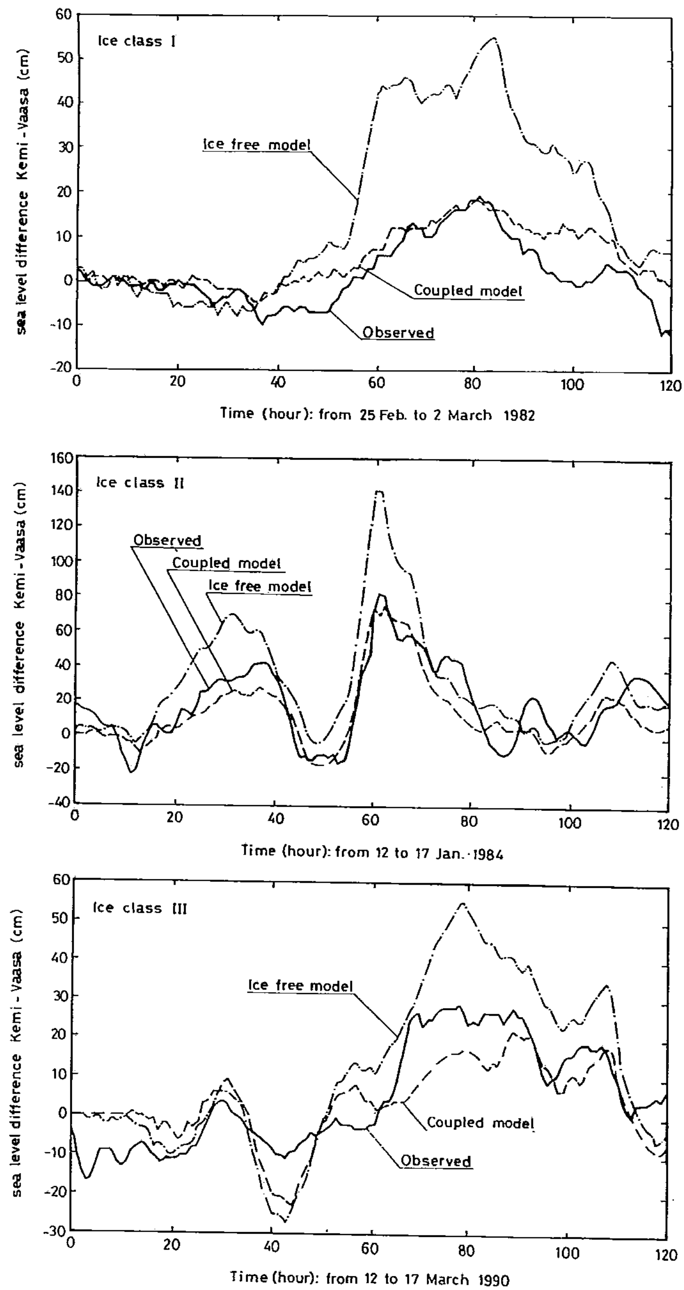

Fig. 7. Sea level differences between Kemi and Vaasa.

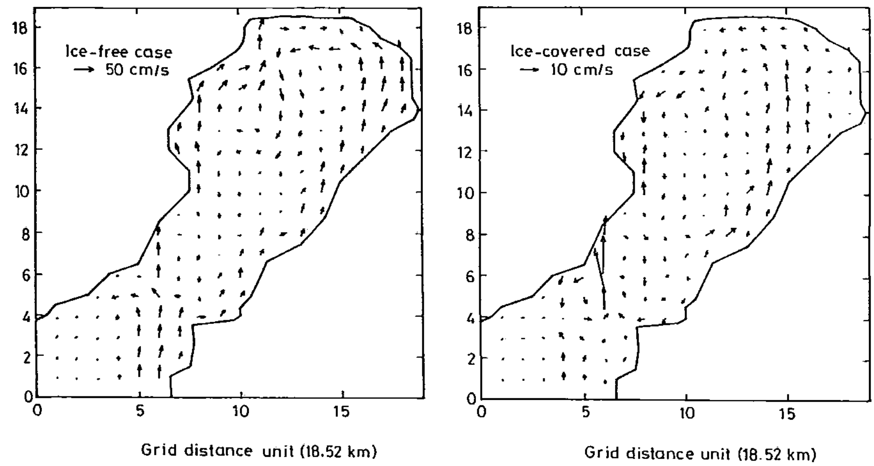

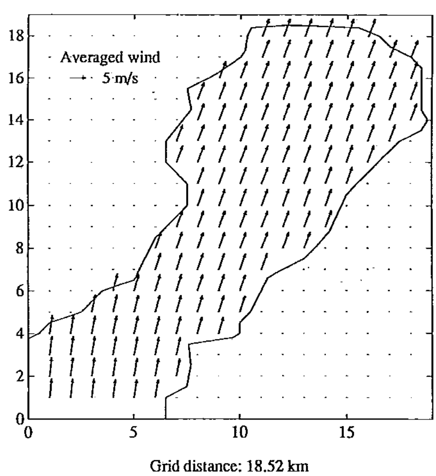

Fig. 8. The depth-averaged current and the wind velocity in the Bay of Bothnia in case 1. The velocities are means over the strongest winds period (24 hours).

4. Conclusions

The influence of sea ice on wind-driven sea level variations has been examined. First simple analytic studies were performed. Then an advanced coupled ice-ocean model was used to simulate the evolution of the sea level in various ice situations.

The results show that variations in the sea level elevation and water piling-up in the Gulf of Bothnia are strongly suppressed in winter due to the presence of ice. The ice cover reduces the sea level variations particularly at low frequencies (less than 0.04 cph). This reducing influence is related to the strength of the ice cover, i.e. ice compactness and thickness. In severe ice situations the sea surface slope may get down to 1/3 of the ice-free value in similar wind conditions. But even in mild ice conditions the reduction is about 2/3. The results agree with observations fairly well. Besides reducing the sea level changes the ice cover also affects the current field. In the severe ice case the modelled current speeds were only 20 percent of the ice free values. Maximum decrease in current velocity was found in the fast ice areas.

In addition, the possibility to use a coupled ice-ocean model for predicting sea level changes in winter was successfully tested. However, while the results for the water piling-up were quite good, the flow details are not well described because a two-dimensional oceanic model was used. A three-dimensional oceanic model would be needed to further study the under-ice current fields in the Baltic Sea.

Acknowledgements

This work is a part of the Chinese-Finnish cooperative research program 'Sea Ice Modeling in Marginal Seas'. It was originated and also much of the modeling work was done in the Finnish Institute of Marine Research; we are grateful to Prof. Pentti Mälkki, director of the Institute for support. We would like to thank Dr. Anders Omstedt, Dr. Leif Nyberg and Dr. Kimmo Kahma for useful discussions, Mr. Jari Haapala for his careful review of the manuscript, and Mr. Donald Smart for checking the English language. Financial support has been obtained from the Finnish Ministry of Trade and Industry and the National Natural Science Foundation of China.

5. References

FIMR, 1982, 1984, 1990: Ice charts over the Baltic Sea. Published twice per week. *Finnish Institute of Marine Research*, Helsinki.

Garratt, J.R., 1977: Review of drag coefficients over oceans and continents. *Mon. Wea. Rev.*, Vol. **105**, 915-929.

Hibler, W.D. III, 1979: A dynamic thermodynamic sea ice model. *J. Phys. Oceanogr.*, Vol. **9(4)**, 815-846.

Joffre, S.M., 1984: The atmospheric boundary layer over the Bothnian Bay; a review of work on momentum transfer and wind structure. *Winter Navigation Research Board*, Res. Rep. No. **40**, Helsinki, Finland, 58 p.

Leppäranta, M., 1981: On the structure and mechanics of pack ice in the Bothnian Bay. *Finnish Marine Research* no. **248**, p. 3-86.

Leppäranta, M. and W.D. Hibler III, 1985: The role of plastic ice interaction in marginal ice zone dynamics. *Journal of Geophysical Research* **90(C6)**, 11899-11909.

Leppäranta, M. and A. Omstedt, 1990: Dynamic coupling of sea ice and water for an ice field with free boundaries. *Tellus*, Vol. **42A**, 482-495.

Leppäranta, M. and Zh.-H. Zhang, 1992: A viscous-plastic ice dynamic test model in the Baltic Sea. *Finnish Institute of Marine Research*, Internal Rep. 1992(3). Helsinki, Finland.

Li, W.-H. and S.-H. Lam, 1964: Principles of Fluid Mechanics. Addison-Wesley, Reading, Mass. 374 p.

Lisitzin, E., 1957: On the reducing influence of sea ice on the piling-up of water due to wind stress. Commentat. Physico-Math. *Soc. Sci. Fenn.*, Vol. **20**, No. 7, 1-12.

Omstedt, A. and L. Nyberg, 1991: Sea level variations during ice-covered periods in the Baltic Sea. *Geophysica* **27(1-2)**: 41-61.

Peaceman, D.W. and H.H. Rachford, Jr., 1955: The numerical solution of parabolic and elliptic differential equations. *J. Soc. Indust. Appl. Math.*, Vol. **3**, No. 1, 28-41.

Zhang, Zh.-H. and M. Leppäranta, 1992: Modeling the influence of sea ice on water in the Gulf of Bothnia. *Finnish Institute of Marine Research*, Internal Rep. 1992(4), 18 p.

Zhang, Zh.-H. and H.-D. Wu, 1990a: Numerical simulation for storm surges in the China Sea. *Marine Forecasts*, Vol. **7**, No. 2, 10-19 (in Chinese).

Zhang, Zh.-H. and H.-D. Wu, 1990b: Trial numerical prediction on extratropical storm surges in the Bohai Sea. *Marine Sci. Bull.*, Vol. **9**, *No. 5, 11-16 (in Chinese).*